

PHYSICAL REVIEW LETTERS

VOLUME 25

28 DECEMBER 1970

NUMBER 26

Relation of Collision-Induced Light Scattering in Rare Gases to Atomic Collision Parameters

J. I. Gersten

City College of the City University of New York, New York, New York 10031

and

R. E. Slusher and C. M. Surko

Bell Telephone Laboratories, Murray Hill, New Jersey 07974

(Received 5 October 1970)

New data and calculations on collision-induced light scattering in rare gases are presented. The theory and experiment are in quantitative agreement. The spectra are found to be approximately piecewise exponentials whose decay constants are directly related to atomic collision parameters.

Collision-induced light scattering (CIS) in atomic gases bears a close relationship to the more familiar Raman effect in molecular gases. In place of permanent molecules, however, one has colliding pairs of atoms. The scattered radiation is depolarized and cast into a broad spectrum of frequencies. By interpreting this spectrum one can obtain information about atomic-collision parameters in an energy range not easily accessible by other methods. These scattering techniques may also be extendible to the study of multiple-body collisions in dense gases and liquids.

In the present article CIS in the rare gases is studied both experimentally and theoretically. The detailed spectral shape is analyzed in terms of atomic properties. We find that typically there appear to be several slopes on a semilogarithmic plot of the spectral intensity. The high-frequency slope is related to the form of the repulsive part of the interatomic potential, $V(R)$, while the lower-frequency slopes reflect the detailed structure of the anisotropic part of the polarizability of a colliding pair, $\beta(R)$, and the attractive part of $V(R)$.

Previous theoretical studies of CIS have focused largely on the qualitative interpretation of

the phenomenon. Thus in the Levine-Birnbaum theory¹ a somewhat artificial model for $\beta(R)$ is invoked and straight-line trajectories are assumed. Their theory predicts that the radiation would be scattered into an exponential spectrum whose slope is related to the inverse duration of a collision. Thibeau and Oksengorn² have extended the theory somewhat by including hard sphere collisions and the correct asymptotic form for $\beta(R)$. The present paper generalizes to realistic forms for $\beta(R)$ and $V(R)$, and properly describes the collision trajectories. Previous experimental investigations of CIS have been made by McTague and Birnbaum.³ While the gross features of these experiments agree with theory, no real quantitative comparison has yet been possible.

Collision-induced Raman spectra for Ar and Kr gas at room temperature are shown in Fig. 1. The dots represent experimental points. These spectra were excited by ~200 mW of linearly polarized 5145-Å Ar laser radiation. Light scattered at 90° with polarization in a plane orthogonal to the incident laser polarization was analyzed by a double spectrometer, detected by a photomultiplier, and digitally averaged over many sweeps using a small computer. Only

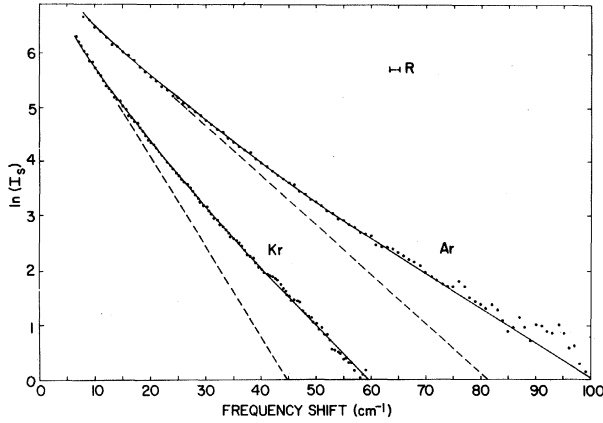


FIG. 1. Experimental and theoretical collision-induced light scattering spectra for Argon (100 atm) and Krypton (50 atm) at $T=300$ K. I_s is the scattered light intensity in arbitrary units. The dots are digitally averaged data, the dashed line is the extension of the initial slope, and the solid lines are theoretical curves adjusted in absolute intensity for best fit.

Stokes scattering was analyzed. The data were digitally corrected for Brillouin, Rayleigh, and "dirt" scattering (most important at small frequency shifts) and for the dark current of the photomultiplier (most important at large frequency shifts). The spectral form was found to be constant for pressures up to 50 atm for Kr and 100 atm for Ar.⁴ For these pressure ranges the integrated intensity was found to vary as the square of the density. This implies that the spectra in Fig. 1 characterize only two-body atomic collisions. At higher pressures the spectral widths begin to increase, probably because of higher-order collisions. The results obtained here are similar in a qualitative way to those obtained previously.³ Our data are more accurate since both elastic scattering and photomultiplier dark current are subtracted using precision digital techniques.⁵ Previously, the spectrum has been interpreted as predominantly a single exponential. Both the Ar and Kr data in Fig. 1 can be approximated by several nearly exponential regions. For each region $I_s \sim e^{-\delta/\Delta}$, where δ is the frequency shift of the scattered light and Δ is the decay constant. We find that $\Delta = 5.9$ ($7 < \delta < 14$), 8 ($14 < \delta < 31$), and 9 ($31 < \delta < 60$) for Kr and $\Delta = 11$ ($7 < \delta < 23$), 13.3 ($23 < \delta < 53$), and 17 ($53 < \delta < 100$) for Ar, where δ and Δ are in cm^{-1} . Extensions of the first slopes are shown as dashed lines in Fig. 1. We will show below that the parameters describing these three regions are directly related to $\beta(R)$ and $V(R)$.

The spectral intensity of the depolarized radia-

tion can be shown to be given by

$$dI/d\Omega = (4\pi/75)I_0 n^2 v (\omega/c)^4 \times \sum_{j=-2}^{+2} |Y_{2j}(\pi/2, 0)|^2 \int b db |I_j|^2, \quad (1)$$

where we have defined a scattering integral

$$I_j = \int_{-\infty}^{\infty} \beta(R) e^{i(\eta t + j\varphi)} dt. \quad (2)$$

In the above, I_0 is the intensity of the incident light, ω is the frequency of the scattered light, $\eta = 2\pi c\delta$, Y_{2j} are spherical harmonics, n is the atomic density, v is the velocity of a colliding pair, and b is the impact parameter. The collision trajectory is described by $R(t)$ and $\varphi(t)$, the radial and azimuthal coordinates. In Eqs. (1) and (2) a classical description is assumed.

The high frequency wings of I_j will be sensitive to the sharpest features in the scattering process. These occur near the turning point of the trajectory. Not only is the trajectory varying most rapidly there but the $\beta(R)$ function is peaking most rapidly also. Thus we introduce a dynamics which is applicable only near the turning point. This must be done in a manner which respects the analytic behavior of a trajectory in the complex time plane. Hence R and φ must be double-branched functions in time. From Newton's second law it can be shown that, through second order in t ,

$$R = r_0 [1 + (t/\xi_0)^2]^{1/2}, \quad (3a)$$

and

$$\sin\varphi = bvt/Rr_0, \quad (3b)$$

where r_0 is the turning radius, and $\xi_0 = (mr_0/F_0)^{1/2}$. Here m is the reduced mass, and F_0 is the sum of the interatomic and centrifugal forces acting at the turning point. The parameter ξ_0 is a measure of the duration of a collision. In the limit as $V(R)$ approaches zero Eqs. (3a) and (3b) reduce to the exact expressions for a straight-line trajectory.

The evaluation of the scattering integral of Eq. (2) may be performed using this pseudodynamics. First a model for $\beta(R)$ must be introduced. We take the following model:

$$\beta(R) = 6\alpha^2(R^{-3} + \rho R^{-6}) = \sum_n \beta_n R^{-n}, \quad (4)$$

where α is the atomic polarizability. The need for the R^{-3} term has long been recognized.⁶ The R^{-6} term is the next term in the multipole series and stems from the second-order dipole-dipole interaction. Higher terms in the multipole series are omitted. To fix the value of the parameter

ρ we evaluate the Kerr constant corresponding to Eq. (4) and compare it with the experimental measurements of Buckingham and Dunmur.⁷ The Kerr constant corresponding to Eq. (4) can be expressed analytically in terms of parabolic cylinder functions.⁸ We find for Ar $\rho = -9.87 \text{ \AA}^3$ and for Kr $\rho = -17.6 \text{ \AA}^3$.

A typical scattering integral may be expressed in terms of modified Bessel functions, K_n . Thus, letting $I_0 = \sum_n \beta_n I_0^{(n)}$, we have

$$I_0^{(n)} = [2\pi^{1/2} \xi_0 / 2^n r_0^{2n+1} \Gamma(n + \frac{1}{2})] (\xi_0 \eta)^n K_n(\xi_0 \eta). \quad (5)$$

The integration over impact parameters implicit in Eq. (1) is more readily performed as an integral over distances of closest approach. Thus we employ the following relation:

$$2\pi b db = (2\pi r_0^2 F_0 / mv^2) dr_0. \quad (6)$$

For the interatomic potential the Lennard-Jones potential was employed. The parameters for Ar were taken to be $\epsilon/k = 119.8 \text{ K}$ and $\sigma = 3.405 \text{ \AA}$, and for Kr $\epsilon/k = 171 \text{ K}$ and $\sigma = 3.60 \text{ \AA}$.³ As a final step a thermal average over relative velocities was performed numerically. The results after this velocity averaging are quite similar to those obtained using the mean thermal velocity except for a slightly sharper rise at low-frequency shifts.

In Fig. 1 the theoretical curves are represented by solid lines. The agreement is quite good. There are no adjustable parameters in the theory. Only the intensities were normalized for comparison in Fig. 1.

A series of calculations was performed to determine the sensitivity of each slope to $V(R)$ and $\beta(R)$. It is found that the high-frequency slope is most influenced by the form of $V(R)$ near the classical turning point. The middle slope is affected considerably by the size of the parameter ρ in Eq. (4). Thus it is an indicator of the short-range part of $\beta(R)$. The low-frequency slope depends on the contribution from distant collisions, and thus is sensitive to the asymptotic parts of $\beta(R)$ and $V(R)$. If one had to make a connection with the Levine-Birnbaum theory¹ it would probably be that the low-frequency slopes should coincide.

The high-frequency slope can be correlated with the location of the branch point of $\beta(R)$ in the upper-half t plane. In fact it is not difficult to show from Eqs. (2), (3), and computer averaging over velocities that this slope is given approximately by $\Delta = \frac{1}{4}\pi c \xi_0$, where ξ_0 is evaluated for a head-on collision at mean thermal velocity (e.g.,

for Ar the calculation shown in Fig. 1 gives $\Delta = 16 \text{ cm}^{-1}$ as compared with $\frac{1}{4}\pi c \xi_0 = 17.1 \text{ cm}^{-1}$). It seems possible to select, on the basis of the experimental high-frequency slope, the most appropriate repulsive potential. Other realistic potential forms give a difference in this slope of approximately $\pm 1 \text{ cm}^{-1}$ which we are able to resolve with our present experimental accuracy. The experimental data for Ar and Kr seem to be adequately described by Lennard-Jones potentials; however, a more precise measurement of the Kerr constant would lead to a more definitive conclusion. It should be pointed out that this technique enables one to study chiefly the repulsive part of the potential at thermal energies, a domain not easily studied by other methods.

As mentioned earlier, the present analysis employed the Kerr constant measurements of Buckingham and Dunmur.⁷ The agreement between theory and experiment indicates that these numbers are sound (despite the uncertainty of nearly 100% quoted for Krypton).⁷ Alternatively, one can invert the problem and employ CIS to measure the Kerr constant. The agreement of theory and experiment also lends support to the assumption that higher multipoles in Eq. (4) are unimportant. An *ab initio* calculation of ρ would be helpful in estimating the contribution of these higher-order terms. Finally it should be pointed out that some of the bumps in the large frequency shift region are reproducible but are not yet understood in detail. For Ar and Kr the effects of dimers do not appear to be important, since the agreement between theory and experiment is very good in the low-frequency region where dimers might be expected to affect the spectrum.

In conclusion, the excellent agreement between theory and experiment obtained here indicates that this technique might be of general use for obtaining atomic collision parameters for spherical atoms and molecules. In principle one could extend the present techniques to anisotropic molecular gases.

We would like to thank Professor A. A. Abrahamson for an informative discussion concerning interatomic potentials and J. Strautins for technical assistance. We also thank P. A. Fleury and D. L. Rousseau for critical reading of the manuscript.

¹H. B. Levine and G. Birnbaum, *Phys. Rev. Lett.* **20**, 439 (1968).

²M. Thibeau and B. Oksengorn, *Mol. Phys.* **15**, 579

(1968).

³J. P. McTague and G. Birnbaum, *Phys. Rev. Lett.* **21**, 661 (1968), and to be published.

⁴At low pressures of Ar and Kr, the damped rotational Raman spectra of impurities (e.g., N₂) can distort the spectral form at large frequency shifts. For the purity of gas used here (less than 10 ppm impurities) these effects were found to be negligible.

⁵For the data in Fig. 1, the error (including system-

atic effects) is estimated to be no larger than the random scatter between adjacent points. For further details concerning the background subtraction see R. E. Slusher, C. M. Surko, and J. Strautins, to be published.

⁶L. Silberstein, *Phil. Mag.* **33**, 521 (1917).

⁷A. D. Buckingham and D. A. Dunmur, *Trans. Faraday Soc.* **64**, 1776, (1968).

⁸J. I. Gersten, to be published.

Picosecond Emission Spectroscopy of Homogeneously Broadened, Electronically Excited Molecular States

P. M. Rentzepis, M. R. Topp, and R. P. Jones
Bell Telephone Laboratories, Murray Hill, New Jersey 07974

and

J. Jortner
Department of Chemistry, Tel-Aviv University, Tel-Aviv, Israel
(Received 10 November 1970)

We present a direct observation of an ultrafast time-resolved emission spectrum of a dye molecule in solution, the time resolution of the system being 2×10^{-12} sec. Vibrational relaxation within the vibrational manifold of the excited electronic state of rhodamine 6G occurs within 6×10^{-12} sec. We discuss the implications of these results for the understanding of homogeneous broadening of excited electronic states of large molecules.

Inhomogeneous line-broadening effects resulting in the broad optical absorption bands for intravalence electronic excitations of large organic molecules in solution can be attributed to two major sources: (a) intramolecular sequence congestion,¹ (b) intermolecular coupling (via linear and quadratic terms in nuclear displacements) of each molecular vibronic level to the lattice² (or rather to the solvent molecules in the nearby environment of the guest molecule). When the molecule is characterized by a significant change in the equilibrium geometry between the two electronic states, then electronic excitation from the ground state will result in a distorted nuclear configuration in the excited electronic state, which subsequently relaxes vibrationally via intramolecular and intermolecular channels. The final result of this relaxation process involves dissipation of vibrational energy to the medium.³ This relaxation mechanism, which for large molecules is believed to be as fast as the time scale of the spontaneous radiative decay,⁴ results in homogeneous line broadening. Until recently, these ultrafast molecular processes were not amenable to experimental study.

The recent development of picosecond pulse

techniques⁵ and the measurements of the pulse duration by two-^{6,7} and three-photon^{8,9} fluorescence methods has initiated studies of ultrafast molecular relaxation processes.¹⁰⁻¹⁶ Up to date, time-resolved experimental methods utilized for picosecond spectroscopy have been based upon averaging of several laser shots¹⁶ at each wavelength to display the "average" time-dependent spectrum. In this note we present what we believe to be the first direct observation of an ultrafast time-resolved emission spectrum of a large organic molecule in solution. A method has been developed for monitoring a time-versus-frequency spectrum by a normal spectrometer. The time resolution is limited by the width of the mode-locked laser pulse and by the rotational relaxation time of the optical shutter. With obvious modifications the time resolution of this system can be less than 10^{-12} sec, while the frequency resolution is strictly spectrometer dependent.

The experiment utilizes as a time-resolving element an optical shutter consisting of a 0.1-mm CS₂ liquid cell located between a pair of crossed polarizers.^{17,18} The shutter is opened by a picosecond pulse of the first harmonic of a Nd³⁺-glass mode-locked laser. The shutter ad-